

White Matter Tract Probability Atlas Derived From Diffusion Tensor Tractography of a Large Population

C. Lebel¹, L. Concha¹, G. Gong¹, and C. Beaulieu¹

¹Biomedical Engineering, University of Alberta, Edmonton, Alberta, Canada

INTRODUCTION: The increasing attention to white matter pathology in a variety of brain disorders has pointed to the need for a comprehensive white matter atlas labeling the location of major white matter fiber bundles in the human brain¹. Previous reports using diffusion tensor imaging (DTI) tractography have shown the variability in the spatial distribution of specific white matter tracts, but are limited by small subject numbers (N=10-28)²⁻⁵. A comprehensive white matter tract atlas encompassing a large number of subjects would be useful not only for exploring intersubject variability of specific white matter structures, but also for facilitating automated tract-specific analysis of MRI parameters and assigning structures to voxels identified as significant using voxel-based analysis methods. The goal of this study was to use DTI tractography to construct a probability atlas demonstrating the spatial distribution and variability of thirteen major white matter tracts in a large cohort of control subjects (N=254).

METHODS: Subjects were 254 healthy volunteers aged 5-58 years (126m/128f, 235 right-handed) with no history of neurological disease or injury. DTI was performed on the same 1.5T Siemens Sonata scanner using dual spin echo EPI, with 40 3mm slices (no gap), image matrix 128x128 zero-filled to 256x256, TE/TR=98ms/6400ms, b=1000s/mm², 8 averages, 6 directions, 6:06 min acquisition. A semi-automated deterministic tractography method (ExploreDTI), in which seeding, inclusion, and exclusion regions were drawn on a homemade template FA map (based on 20 scans of one 25 year old male subject) and automatically mapped to native space for each individual, was used to reconstruct 13 major white matter tracts: the genu, body, and splenium of the corpus callosum (gCC, bCC and sCC, respectively), superior and inferior longitudinal fasciculi (SLF and ILF), superior and inferior fronto-occipital fasciculi (SFO and IFO), uncinate fasciculus (UF), temporal and supra-callosal portions of the cingulum (tCing and sCing), the anterior limb and posterior limb of the internal capsule (ALIC and PLIC) and the fornix (Fx). Binary tract masks were created for each individual for each tract in native space, and normalized (using deformation parameters from b0 image to EPI template) to the Montreal Neurological Institute (MNI) space using a non-linear transformation (implemented using the SPM5 software package). Probability maps were then calculated for each voxel of every tract by determining the number of subjects in whom a particular voxel contained that tract. These were then combined to produce a thirteen-tract white matter atlas containing the probability of each tract occurring in each voxel across the entire brain.

RESULTS/DISCUSSION: Tract probability maps are shown for several axial slices in Fig.1, and illustrate the frequency of occurrence of each tract in each voxel. For any given voxel, only the tract with the highest probability of occupying that space is shown. As expected, the core of each tract shows a very high probability of tract occurrence, compared to low probabilities at the periphery of each tract. As shown in Fig.2, some tracts, such as the corpus callosum, have high spatial overlap across subjects (as high as 95-97%), while other tracts, such as the supra-callosal and temporal cingulum and the PLIC, are more variable (highest probability of overlap is 72, 75 and 80%, respectively). All tracts had some voxels with at least 70% overlap. Fig.2B shows contour lines representing the area of 70% (yellow) and 30% (red) overlap within several tracts. The corpus callosum (blue) and the SLF (green) demonstrate small core regions of high probability in this slice, while tracts such as the cingulum and fornix show only regions with 30% overlap, and the PLIC does not even reach 30% overlap in this slice.

The small region of high probability and the large region of low probability for each tract suggest that considerable intersubject variability exists, even after non-linear normalization. This likely indicates that the centre of a tract is the most reliable location to look for differences using a voxel-based approach (this is the rationale behind tract-based spatial statistics⁶), whereas voxels in the periphery of tracts may truly represent that specific structure in only a small percentage of individuals. These atlases could be used to infer the structures underlying voxel-based analyses, while providing an estimate of certainty for the structures involved. Since the brain is known to undergo structural age-related changes, creating atlases with a subgroup of subjects representing more specific populations (e.g. 8-12 year old children, right-handed females over 30 years) may reduce the variability and improve overlap within tracts. In conclusion, we have established a tract-based white matter tract atlas based on a large number of subjects across a wide age range that can be used for determining location and variability of major white matter tracts, examining tract-specific parameters, and producing custom atlases based on subgroups of specific populations.

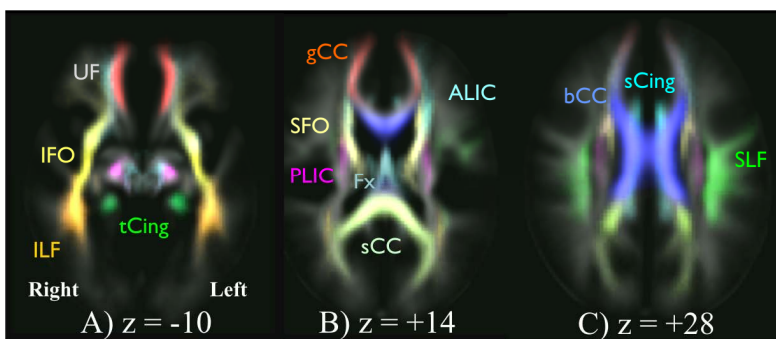


Figure 1. Spatial probability distribution of white matter tracts in standard (MNI) space, axial sections, shown on the mean FA map of all subjects. The intensity in each pixel represents the probability of a certain tract occupying that pixel; the tract's color is arbitrary. The core of most tracts show high degree of overlap amongst individuals, which quickly fades towards the edges of the tracts

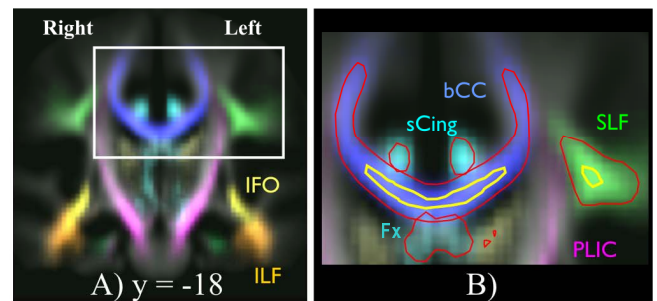


Figure 2. Coronal sections of the probability distribution of white matter tracts. The zoomed region in B shows iso-probability lines at 30% (red) and 70% (yellow). The body of the corpus callosum and the SLF show areas of high probability, whereas the cingulum and PLIC have overall low degree of overlap amongst individuals.

REFERENCES: 1. S Wakana *et al.*, *Radiology* **230**, 77 (2004). 2. K Hua *et al.*, *Neuroimage* (2007). 3. U Burgel *et al.*, *Neuroimage* **29**, 1092 (2006). 4. P Thottakara *et al.*, *Neuroimage* **29**, 868 (2006). 5. O Ciccarelli *et al.*, *Neuroimage* **19**, 1545 (2003). 6. SM Smith *et al.*, *Neuroimage* **31**, 1487 (2006).